

# Phase-Amplitude Representation of Continuum States

Daniel Hadush\* and Charles Weatherford†

*Physics Department, Florida A&M University, Tallahassee, FL, USA*

(Dated: January 22, 2025)

arXiv:2501.10797v1 [quant-ph] 18 Jan 2025

## Abstract

A numerical method of solving the one-dimensional Schrödinger equation for the regular and irregular continuum states using the phase-amplitude representation is presented. Our solution acquires the correct Dirac-delta normalization by wisely enforcing the amplitude and phase boundary values. Our numerical test involving point-wise relative errors with the known Coulomb functions shows that the present method approximates both the regular and irregular wavefunctions with similar, excellent accuracy. This is done by using new basis polynomials that, among other advantages, can elegantly enforce the derivative continuity of any order. The current phase-amplitude method is implemented here to study the continuum states of Coulomb-screened potentials. We discovered that, during the parametric transition from a Hydrogen atom to the Yukawa potential, the electronic density at the origin exhibits surprising oscillation - a phenomenon apparently unique to the continuum states.

## I. INTRODUCTION

Wavefunctions of an electron in a continuum state oscillate like the trigonometric sine and cosine functions as the effect of the potential fades out at infinity. This behavior contrasts with their bound state counterparts, which decay exponentially after a few oscillations near the origin. This inherent oscillation makes the numerical computation of continuum states time-consuming and prone to errors. They are also not square integrable, meaning numerical integration cannot determine their normalization. However, it has long been established that both of these issues can be efficiently addressed if one were to instead solve for the amplitude and the phase of the continuum states, both of which are universally simple, monotonic functions [1, 2]. The amplitude can also be appropriately written so that it flattens into a constant at infinity (away from the potential effects). This constant can be used to set the normalization.

However, the governing equations for the phase-amplitude representation are nonlinear and numerically challenging, given that their solutions are deceptively simple. In their attempt to solve these equations, researchers are mostly faced with a treacherous effort

---

\* daniel.hadush@fam.u.edu

† charles.weatherford@fam.u.edu

involving several trials to exhaust all reasonable options. In addition to solving the differential equation (DE), the amplitude must have proper normalization and the phase proper synchronization to be valid. Despite the numerous literature on the topic, clear evidence has not yet been reported that specifies a successful numerical computation [3–5].

The path toward the solution presented in this work is the best we could achieve after exhausting several options, and its outcome is portrayed by the point-wise relative errors for the Coulomb functions, one of the rare systems with known analytic solutions.

Electronic density at the origin of the Coulomb-screened potentials is also studied in this work for the first time in light of the continuum states. The bound state counterparts have been reported by the authors recently [6], and this work can be considered a continuation of that study. The discussion begins with the tools that will be used in the numerical computation, and then a schematic derivation of the working DEs and detailed steps on how to solve them will be given. Discussions on numerical examples, plots, and tables will also be presented, followed by conclusions.

## II. TRANSLATION OPERATOR

The translation operator  $e^{\mathbf{x} \cdot \nabla_{\mathbf{a}}}$  in linear algebra translates a function  $f$  of  $m$  variables from point  $\mathbf{a}$  to point  $\mathbf{a} + \mathbf{x}$  [7].

$$f(\mathbf{a} + \mathbf{x}) = e^{\mathbf{x} \cdot \nabla_{\mathbf{a}}} f(\mathbf{a}) = \sum_{n=0}^{\infty} \frac{(\mathbf{x} \cdot \nabla_{\mathbf{a}})^n}{n!} f(\mathbf{a}) \quad (1)$$

We have used a boldface font for an  $m$ -dimensional vector  $\mathbf{x} = (x_1, x_2, \dots, x_m)$ . As shown above, the definition is also equivalent to the Taylor’s expansion of the function  $f(\mathbf{a} + \mathbf{x})$  about a fixed point  $\mathbf{a}$ . Expanding the dot product of the differential operator in the Cartesian coordinate system as  $(\mathbf{x} \cdot \nabla_{\mathbf{a}}) = \sum_{i=1}^m x_i (d/da_i)$ , using the multinomial expansion of its  $n^{\text{th}}$  power, and substituting into Eq. (1), one can write

$$f(\mathbf{a} + \mathbf{x}) = \sum_{n=0}^{\infty} \sum \left[ \left( \frac{x_1^{n_1}}{n_1!} \frac{d^{n_1}}{da_1^{n_1}} \right) \left( \frac{x_2^{n_2}}{n_2!} \frac{d^{n_2}}{da_2^{n_2}} \right) \cdots \left( \frac{x_m^{n_m}}{n_m!} \frac{d^{n_m}}{da_m^{n_m}} \right) \right] f(\mathbf{a}) \quad (2)$$

where the inner summation is over all different combinations of non-negative integers  $n_1, n_2, \dots, n_m$  with  $\sum_{i=1}^m n_i = n$ . Hence, new basis polynomial functions, termed by us ‘Taylor’ basis (TB) polynomial, defined in Appendix A, naturally emerge from Eq. (2). Their implementation here will be in the numerical approximation of functions locally, in

the finite region near point  $\mathbf{a}$ , by writing the finite form of Eq. (2) in terms of the TB as shown below.

$$f(\mathbf{a} + \mathbf{x}) = \sum_{n=0}^{N-1} \sum [T_{n_1}(x_1)T_{n_2}(x_2) \dots T_{n_m}(x_m)] C_{n_1 n_2 \dots n_m}, \quad N = 1, 2, \dots \quad (3)$$

This expansion's principal significance is that the coefficients  $C$  are numerically the higher order derivatives of  $f$  at  $\mathbf{a}$ , i.e.,  $C_{n_1 n_2 \dots n_m} = [d^{(n_1 n_2 \dots n_m)} / da^{(n_1 n_2 \dots n_m)}] f(\mathbf{a})$ . The parametric dependence of the  $C$ 's on  $\mathbf{a}$  is not explicitly shown above to avoid clutter. One can also drop  $\mathbf{a}$  from the equation entirely once the variable  $\mathbf{x}$ 's locality to the fixed point  $\mathbf{a}$  is implicitly understood.

Thus, the TBs are very convenient for implementing boundary conditions in applications based on finite elements or volume. This precise definition of the coefficients  $C$  also implies that their numerical value is closely related to, or is consistent with, the underlying physical model. Moreover, the association of the rapidly growing factorials with the TB leaves the  $C$ 's with a rather uniform and intuitive numerical behavior, even for a high-order expansion. They are better suited for the collocation method, especially in contrast with the ordinary power function  $x^n$ , as it is well known that the latter leads to a Vandermonde matrix, which is an ill-conditioned matrix [8, 9].

The outer summation on  $n$  above specifies an order of expansion equivalently meaningful in any dimension. It is a means by which we can systematically increment the order of Taylor's series representation of the translation operator by including the batch of terms according to the inner sum in Eq. (3), whose count for each  $n$  is known to be  $\binom{n+m-1}{m-1}$  [10]. Equivalently, the total number of terms in the expansion for a given  $N$  is  $\frac{N}{m} \binom{N+m-1}{m-1}$ . The term in braces in the last two expressions is the binomial coefficient.

### A. One-dimensional Expansion

In this section, we will describe a spectral element method on how the TB can be used to solve a homogeneous differential operator of type  $\hat{S}(x)f(x) = 0$  for a local variable  $x$  corresponding to a point inside a segment  $[a, b]$  such that  $0 \leq x \leq b-a$ . The one-dimensional case will be written for the current purpose as

$$f(x) = \sum_{n=0}^{\nu-1} T_n(x)C_n + \sum_{n=\nu}^{N-1} T_n(x)C_n. \quad (4)$$

The first  $\nu$  of the coefficients  $C$  are assumed to be known from the boundary condition at point  $a$ , i.e,  $C_n = f^{(n)}(a)$ . Combined with the collocation method, this typically leads to a set of simultaneous equations shown element-wise below.

$$\sum_{n=\nu}^{N-1} S_{mn} C_n = F_m, \quad m = 0, 1, \dots, N - \nu - 1 \quad (5)$$

where

$$S_{mn} = \left[ \hat{S}(x) T_n(x) \right]_{x=x_m}, \quad \text{and} \quad F_m = - \sum_{n=0}^{\nu-1} S_{mn} f^{(n)}(a). \quad (6)$$

The collocation point  $x_m$  is the  $(m + 1)^{\text{th}}$  node of the Legendre polynomial of order  $N - \nu$  that is properly mapped onto  $[0, b - a]$ . The value of  $\nu$  depends on the order of the DE in question. For a second-order DE, for instance,  $\nu = 2$  because we must enforce the continuity of the function and its first derivative across the boundary of consecutive finite elements. The notable exception is the very first element, where it suffices to set only  $f(a)$  since any function is of zeroth order from the discontinuous direction of an endpoint.

### III. PHASE-AMPLITUDE REPRESENTATION

In this work, we shall use an alternate representation of the regular and irregular continuum wavefunctions, to be denoted here as  $S_l(r)$  and  $C_l(r)$ , respectively, with the following phase-amplitude *ansatz*

$$S_l(r) = A_l(r) \sin [\Phi_l(r)] \quad (7)$$

$$C_l(r) = A_l(r) \cos [\Phi_l(r)], \quad (8)$$

with inverse relations,

$$A_l(r) = \sqrt{S_l^2(r) + C_l^2(r)} \quad (9)$$

$$\Phi_l(r) = \tan^{-1} \left[ \frac{S_l(r)}{C_l(r)} \right] \quad (10)$$

where  $A$  &  $\Phi$  are the amplitude and phase functions, respectively. An immediate consequence of the above representation is obtained by taking a derivative of Eq. (10)

$$\frac{d}{dr} \Phi_l(r) = \frac{W_l(r)}{A_l^2(r)} \quad (11)$$

where we have recognized the Wronskian as  $W_l(r) = C_l(r)\dot{S}_l(r) - S_l(r)\dot{C}_l(r)$ . The overhead dot represents the derivative with respect to the argument. For the radial form of the Schrödinger equation, which is homogeneous second-order DE,  $W$  is solely dependent on the coefficient of the first-order term. This makes Eq. (10) fundamental because it remains true even without stating the potential.

We begin discussing a quantum mechanical system with the reduced form of the radial equation for an electron in a continuum state under a potential  $V(r)$

$$\ddot{\psi}_l(r) + Q_l(r)\psi_l(r) = 0 \quad (12)$$

where

$$Q_l(r) = k^2 - \frac{l(l+1)}{r^2} - 2V(r). \quad (13)$$

Atomic units will be used throughout. The standard wavefunction will be denoted by the capital  $\Psi_l(r)$ , where its related to its reduced form shown above as  $\psi_l(r) = r\Psi_l(r)$ . The total energy of the system  $E$  is written in terms of the momentum number  $k = \sqrt{2E}$ . The wavefunction  $\psi$  represents either of the regular  $S$  or irregular  $C$  functions. One of the advantages of using the reduced form is, from what is commonly referred to as Abel's identity [11], the resulting  $W$  takes its simplest form: a constant. Moreover, at infinity, the amplitude asymptotically goes to a constant while the two continuum solutions it envelopes behave like the trigonometric sine and cosine functions. For wavefunctions normalized in the energy scale [12, 13]

$$\int_0^\infty \psi_l(E, r)\psi_l(E', r)dr = \delta(E - E'), \quad (14)$$

their correct values are  $W_l(r) \equiv W = 2/\pi$  and  $\lim_{r \rightarrow \infty} A_l(r) = \sqrt{2/(k\pi)}$ . These two values are fundamental to calculating appropriately normalized solutions. Momentum normalized  $\delta(k - k')$  solutions can be obtained by multiplying with  $\sqrt{k}$  [14]. In all of the examples in this article,  $k = 1$  is used to avoid ambiguity.

To find the DE for the amplitude, we differentiate Eq. (7) twice, substitute the regular solutions into Eq. (12), and group the resulting terms into factors of  $\sin \Phi$  and  $\cos \Phi$ . Demanding that all the terms that are factors of the cosine vanish gives  $A\ddot{\Phi} + 2\dot{A}\dot{\Phi} = 0$ , for which Eq. (11) with a constant  $W$  is a solution. Doing the same with the factors of the remaining sine terms and using Eq. (11) gives the following nonlinear DE, commonly known

as Milne DE [1].

$$\ddot{A}_l(r) + Q_l(r)A_l(r) = \frac{W^2}{A_l^3(r)} \quad (15)$$

In most literature, the numerator on the right-hand side has been written as some constant, mostly  $k^2$ , or its numerical value [5, 12, 15]. For clarity, we have explicitly written out the quantity it represents, the Wronskian, instead of its actual value.

The solutions  $A$  and  $\Phi$  are considered valid only if they are appropriately normalized and can attain both triangular legs  $S$  and  $C$  with similar accuracy. The best way to enforce normalization will be to integrate in reverse direction after an appropriate variable change. In this work,  $\rho = 1/r$ , where  $0 \leq \rho < \infty$  is implemented. Unfortunately, the resulting DE of the amplitude in the new variable  $\rho$  becomes even more nonlinear and, according to our experience, difficult to solve in a stable manner. A possible remedy is to solve instead for the amplitude squared  $Y$  or  $A_l(r) = \sqrt{Y_l(r)}$ . It is easy to show that a direct substitution into Eq. (15) gives the following nonlinear DE.

$$\ddot{Y}_l(r) + 2Q_l(r)Y_l(r) = \frac{1}{2Y_l(r)} \left[ \dot{Y}_l^2(r) + (2W)^2 \right] \quad (16)$$

It has also been reported that  $Y$  obeys the following linear DE, which is third order and requires knowledge of the derivative of the potential  $V$  [5, 15].

$$\ddot{Y}_l(r) + 4Q_l(r)\dot{Y}_l(r) + 2\dot{Q}_l(r)Y_l(r) = 0 \quad (17)$$

The above two DEs are readily solvable in the  $\rho$  coordinate. The outline of the steps will be summarized below.

### A. Amplitude

After rewriting the above two DEs in terms of  $\rho = 1/r$  and dividing the  $\rho$ -axis into finite elements,  $Y$  can be integrated out for  $\rho \geq 0$  using the method described in II A. The integration must stop at some  $\rho = r_{\min}^{-1}$  because  $Y$  (due to the irregular  $C$ ) is singular at  $r = 0$ . A prerequisite for an upper limit of  $r_{\min}$  will be given below shortly. For the first element, simply use  $\nu = 1$  and fix  $C_0 = 2/(k\pi)$ , which takes care of the normalization. This is convenient because the higher derivatives of  $Y(r)$ , which were all zero at  $r = \infty$ , change non-trivially for  $\rho = 0$  upon conversion. However, we do not need to find out their value to start the integration here, which is advantageous over other methods that do. This is

true for ordinary DE solvers that are naturally first-order and must cast higher order DEs into a matrix form. For the rest of the following elements,  $\nu = 2$  and  $3$  shall be used for Eq. (16) & Eq. (17), respectively. Since Eq. (16) is nonlinear, it must be solved iteratively where the nonlinear terms on the right-hand side are recovered from the previous iteration. Convergence can be expedited by seeding the coefficients  $C$ , as defined, with the respective derivatives of the solution at the endpoint of the previous element, thus setting the iteration off to a very good start.

## B. Phase

Phase  $\Phi$  is a monotonic function that gains an amount of  $\pi$  at every node of  $S$  (or  $C$ ). Therefore, it is only intuitive to set, by convention, its lowest value at the origin. In our case,  $\Phi_l(r = 0) = 0$  since we are considering the reduced form of the solution. After  $Y$  is known, part of the first element near  $\rho = 0$  does not hold a valid information about  $\Phi$  because the distance has artificially been made finite. The integration of  $\Phi$  must be done in the forward direction, as written in Eq. (11), which confronts us with the synchronization problem of determining the integration constant. A reliable and versatile option is to exploit the fact that given the above convention,  $\Phi_l(r_\pi) = \pi$  can be used where  $r_\pi$  is the first root of the regular solutions  $S$ . Then the phase will simply be

$$\Phi_l(r) = \pi + W \int_{r_\pi}^r \frac{dx}{Y_l(x)}. \quad (18)$$

A regular solution with arbitrary normalization is readily solvable numerically using, for instance, the recently developed first-order forms of the radial equation [6] and some of the techniques discussed in this article. The additional work this entails is rewarded by an accurate value of  $r_\pi$  thanks to the available, excellent root-finding algorithms such as the Newton-Raphson method. Remember, we already need to resort to other methods if we are interested in  $S$  from  $0$  to  $r_{\min}$ . This also implies a new upper limit on the choice of  $r_{\min}$ , namely  $r_{\min} < r_\pi$ .

## C. Regular and Irregular Solutions

Once  $Y$  and  $\Phi$  are obtained, for  $r \geq r_{\min}$ , the regular and irregular solutions can simply be calculated by dropping the two legs of the hypotenuse  $A$  according to Eq. (7) & Eq. (8),



respectively. When the phase is appropriately synchronized, its  $\sin(\Phi)$  and  $\cos(\Phi)$  will be equally correct, such that  $S$  &  $C$  are obtained with identical accuracy. We are now also in a position to get the normalization constant for the regular solution calculated above to obtain  $r_\pi$  and use the resulting, properly normalized  $S$  in the region that extends to the origin ( $0 \leq r \leq r_\pi$ ). In this sense, how below  $r_\pi$  one would like to lower  $r_{\min}$  is motivated entirely by the less common irregular solutions  $C$ .

#### IV. EXAMPLE: SCREENED COULOMB POTENTIALS

As a check, we calculated the regular and irregular Coulomb functions  $V(r) = -Z/r$ , for which analytic solutions are known and are commonly available in scientific libraries [10, 16, 17]. For each finite element, the order of the TB polynomials  $T$  in Eq. (4) is set as  $N = \nu + 12$ . For demonstration,  $r_{\min} = 0.001$  is also used. The resulting relative errors of the states  $s, p, \dots$ , belonging to the first few angular quantum numbers are shown in Figs. 1 & 2.

Strictly speaking, the plots are produced from the linear Eq. (17). Our output from the non-linear Eq. (16) (not shown here) is qualitatively similar overall, with errors that are not worse than by an order of magnitude. The traditional method is used to calculate the regular solutions in the inner segment  $r < r_\pi$  to depict a pragmatic implementation, which explains the improved accuracy fashioned in Fig. 1. The two plots are otherwise similar, characteristic of a well-synchronized phase. This can be imposed as a sanity check on the  $\Phi$  in similar applications. Reference values are taken from [17].

Now that we can calculate the normalized continuum states with the demonstrated accuracy, we would like to report a subtle phenomenon in a closely related system, that comes to light only with sound numeric output. Specifically, the electronic density of the Yukawa potential and its close relations, the bound state of which were studied by us recently(REF): the Yukawa or static screened Coulomb potential (SCP), exponential cosine screened Coulomb potential (ECSCP), and Hulthén potential (HP)

$$V(r) = \begin{cases} -\frac{Ze^{-\alpha r}}{r} & \text{for SCP,} \\ \frac{e^{-\alpha r}}{(1+e^{-\alpha r})} \frac{Z\alpha}{\tanh(-\alpha r/2)} & \text{for HP,} \\ -\frac{Ze^{-\alpha r}}{r} \cos \alpha r & \text{for ECSCP.} \end{cases} \quad (19)$$

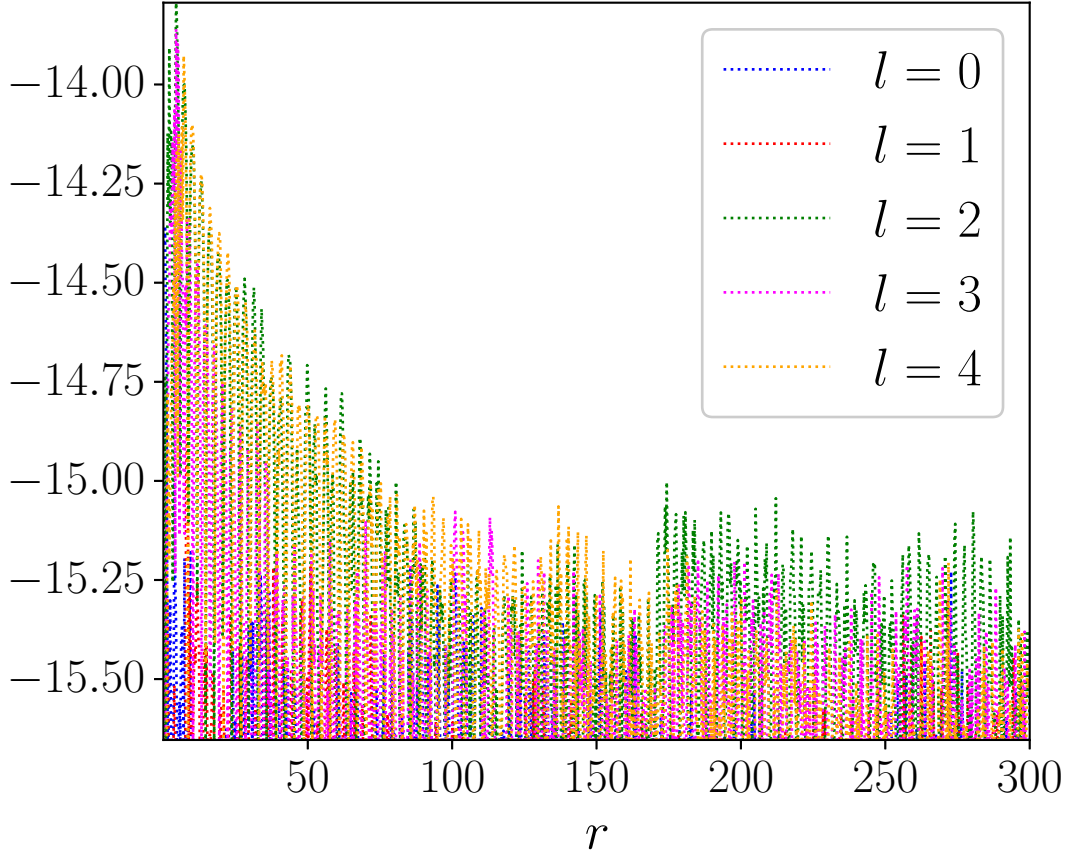


FIG. 1. (Color online)  $\log_{10}$  of relative error of  $l \leq 4$  states of the regular Coulomb functions for  $0.001 \leq r \leq 300$ .

Only  $Z = 1$  is used. The screening parameter  $\alpha \geq 0$  links all of the above three systems to the hydrogen atom at  $\alpha = 0$ . The bound states of the above three systems, specifically, how the ground state energy and the electronic density at the origin vary as  $\alpha$  runs from zero to its critical value, where a bound state can no longer be supported, have been studied recently. In this article, a similar study is done with the electronic density at the origin, here  $\Psi_0^2(0)$ , but for the continuum states. These are shown in a separate plots in Figs. 3 & 4 to zoom in on the peculiar oscillation of the density exhibited by small  $\alpha$ . We expected this particular quantity to decrease monotonically, much like it does in Fig. 4, or in a similar fashion to its bound counterpart. Instead, we obtained the single oscillation shown in Fig. 3. This phenomenon is interesting because it happens for small  $\alpha$ , just as the system leaves the  $H$  atom and not near the critical value. It is not clear what causes its shape or why it does not repeat elsewhere. For reference purposes, representative benchmark values  $\Psi_0(0)$

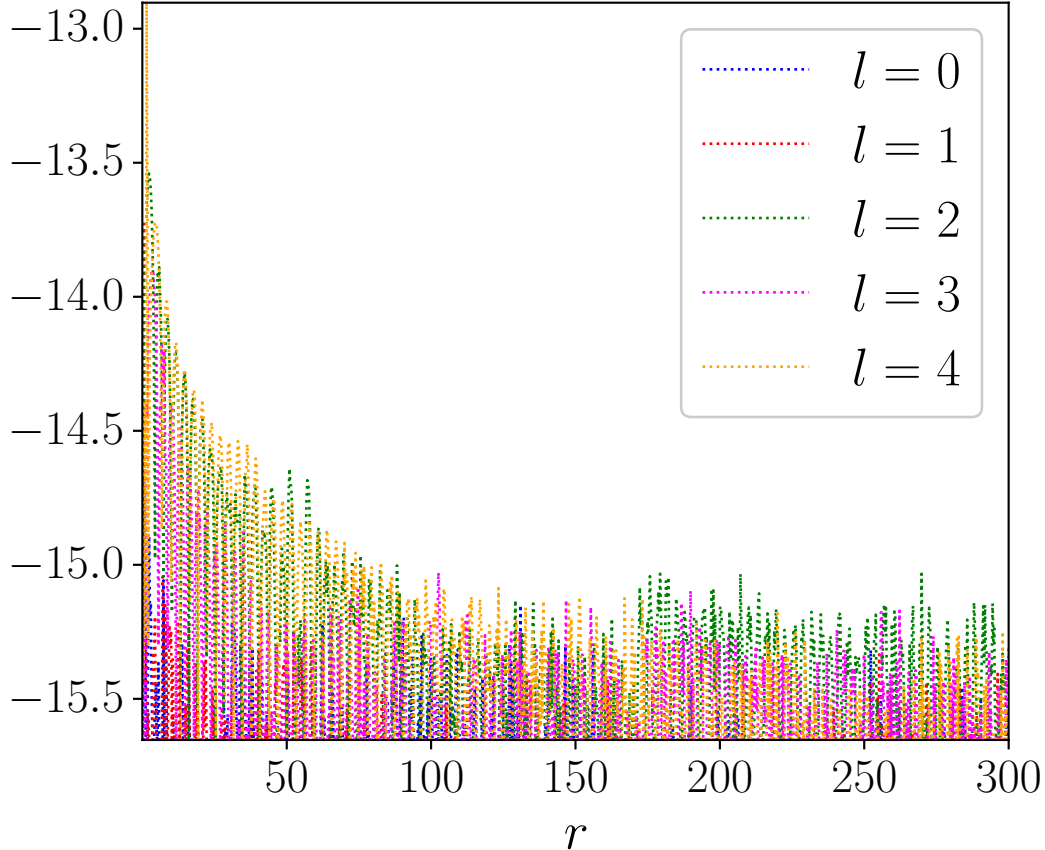


FIG. 2. (Color online)  $\log_{10}$  of relative error of  $l \leq 4$  states of the irregular Coulomb functions for  $0.001 \leq r \leq 300$  as calculated from Eq. (8). The integration was done from left to right.

for the three potentials, including their maximum values, are given in Table I.

All of the plots in this article comprise 1025 uniform data points each.

## V. CONCLUSIONS

The viable path for solving continuum systems using the powerful phase amplitude representation presented here should be sufficient for most applications in electronic structure calculations and can serve as a template. Both of the second and third order DEs for amplitude can be integrated in just a few steps using the included algorithm based on the spectral method within the finite elements. They enable us to arrive at regular and irregular solutions with identical accuracy simultaneously.

TB polynomials are easy to understand and possess properties given in Appendix A that

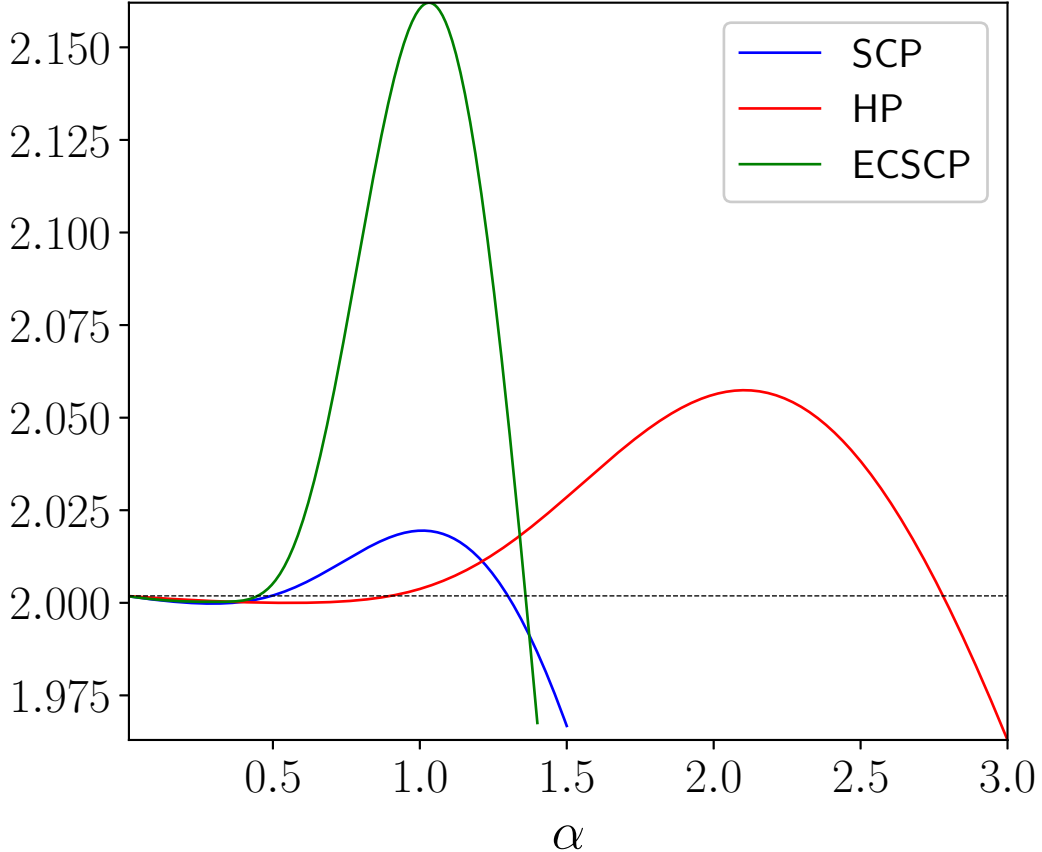


FIG. 3. The normalized  $1s$  state wavefunction at the origin versus  $\alpha$  for the indicated Coulomb screened potentials. The dotted horizontal line is at 2.001 870 062 315 39 for the limiting case  $\alpha = 0$  (Hydrogen atom). The plots are for  $\alpha \geq 0.01$  and  $k = 1$ .

are evidently convenient to implement. The direct connection of the expansion coefficients with the gradient operator makes them a powerful tool for enforcing derivative continuity of arbitrary order across boundaries or for accurate initialization of iterative schemes. Since they stem from the basic translation operator, their potential utility in other avenues deserves more attention, especially in higher dimensional applications.

What is also worth attention to is the oscillation phenomenon of the electronic density at the origin presented, which is observable only with accurately normalized solutions. It should be further understood and put into perspective with other parameterized systems. The behavior of this simple physical quantity affirms that a parametric transition between two physical regimes is not always a smooth sail and perhaps not necessarily intuitive.

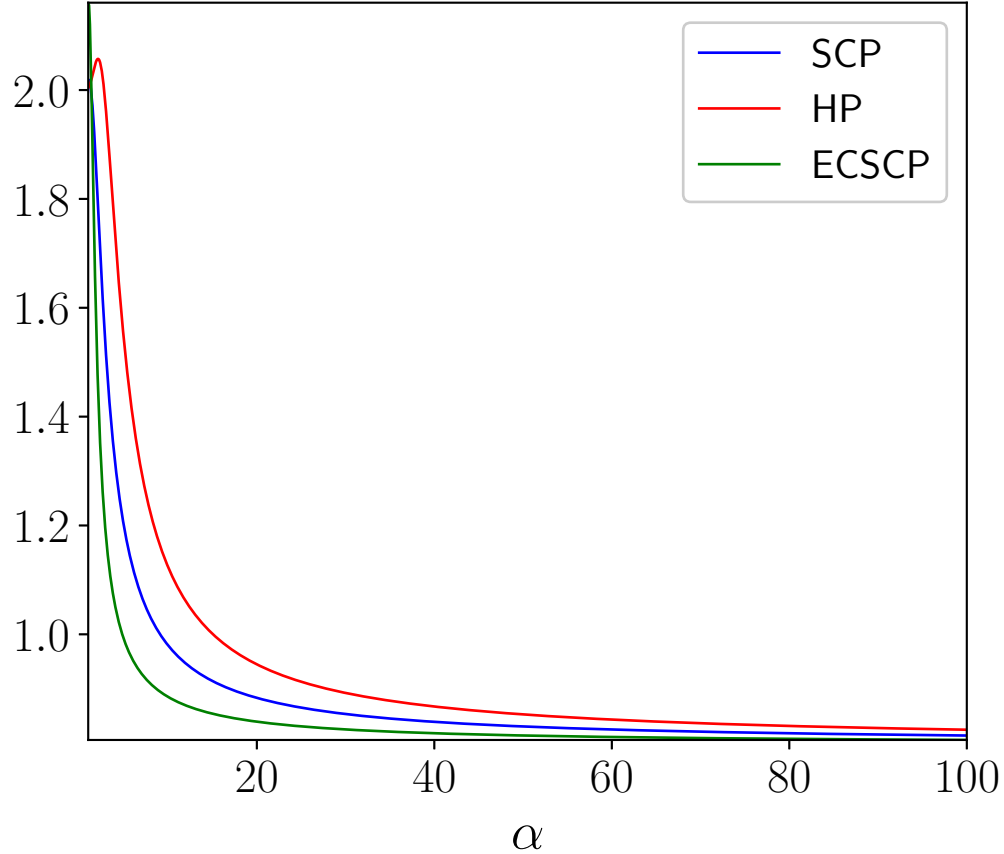


FIG. 4. (Color online) A continuation of Fig. 3 for  $1 \leq \alpha \leq 100$ .

## ACKNOWLEDGMENTS

D.H. and C.W. were partially supported by the Department of Energy, National Nuclear Security Administration, under Award Number (s) DE-0003984.

## Appendix A: Taylor Basis Polynomials

For a real number  $x$ , the ‘Taylor’ basis (TB) polynomial functions are defined as

$$T_n(x) = \frac{x^n}{n!}, \quad n = 0, 1, 2, \dots \quad (\text{A1})$$

where  $n!$  is the factorial function. They obey a simple two-term recurrence formula

$$T_n(x) = \frac{x}{n} T_{n-1}(x), \quad T_0(x) = 1. \quad (\text{A2})$$

TABLE I. Electronic density at the origin,  $\Psi_0^2(0)$ , for the regular  $1s$  continuum state and  $k = 1$  of the Coulomb screened potentials. The underlined figures given in the lower half of the table show the coordinates for the peak points in Fig. 3

$\alpha$	$\Psi_0(0)$		
	SCP	HP	ECSCP
0.01	2.001 753 468 852 04	2.001 811 569 983 04	2.001 754 351 507 03
0.1	2.000 812 154 698 96	2.001 317 067 239 68	2.000 899 143 538 91
1	2.019 489 044 554 80	2.003 738 379 326 01	2.160 510 127 337 48
10	0.979 691 498 590 326	1.123 708 852 625 44	0.885 015 629 968 403
100	0.814 064 055 523 049	0.824 743 905 140 524	0.805 927 073 382 779
<u>1.008 625 496 800 67</u>	<u>2.019 501 542 762 27</u>	2.003 944 948 800 74	2.161 241 023 924 67
<u>2.104 242 184 705 96</u>	1.785 741 131 308 62	<u>2.057 415 252 014 99</u>	1.451 864 737 136 60
<u>1.031 378 946 011 15</u>	2.019 411 732 469 42	2.004 526 760 324 64	<u>2.162 061 665 512 45</u>

Differentiation and integration operations act as the ladder (lowering and raising) operators in quantum mechanics as shown below.

$$\frac{d}{dx}T_n(x) = T_{n-1}(x), \quad \int_0^x T_n(y) dy = T_{n+1}(x) \quad (\text{A3})$$

Their product is another TB of higher order scaled by a binomial coefficient.

$$T_m(x) T_n(x) = \binom{m+n}{n} T_{m+n}(x) \quad (\text{A4})$$

Finally, their addition formula is given by

$$T_n(x+y) = \sum_{m=0}^n T_m(x) T_{n-m}(y). \quad (\text{A5})$$

- 
- [1] W. E. Milne, The numerical determination of characteristic numbers, Phys. Rev. **35**, 863 (1930).
- [2] J. A. Wheeler, Wave functions for large arguments by the amplitude-phase method, Phys. Rev. **52**, 1123 (1937).

- [3] G. Rawitscher, Tunneling through a barrier with the phase-amplitude method, *Computer Physics Communications* **203**, 138 (2016).
- [4] B. Ritchie and A. K. Bhatia, Phase-amplitude solution of the schrödinger equation with application to free-free absorption, *Phys. Rev. E* **69**, 035402 (2004).
- [5] D. Shu, I. Simbotin, and R. Côté, Integral representation for scattering phase shifts via the phase-amplitude approach, *Phys. Rev. A* **97**, 022701 (2018).
- [6] D. Gebremedhin and C. Weatherford, First-order differential equations for single-particle quantum mechanical systems, *Phys. Rev. E* **108**, 045301 (2023).
- [7] F. Jordan, *Linear Operators for Quantum Mechanics* (Dover Publications, Mineola, NY, 1969) pp. 121–122.
- [8] H. Golub and F. van Loan, *Matrix Computations*, 4th ed. (The Johns Hopkins University Press, 2013) pp. 203–207.
- [9] W. H. Press, S. A. Teukolsky, W. T. Vetterling, and B. P. Flannery, *Numerical Recipes 3rd Edition: The Art of Scientific Computing*, 3rd ed. (Cambridge University Press, New York, NY, USA, 2007).
- [10] F. W. Olver, D. W. Lozier, R. F. Boisvert, and C. W. Clark, *NIST Handbook of Mathematical Functions*, 1st ed. (Cambridge University Press, New York, NY, USA, 2010).
- [11] S. Hassani, *Mathematical Physics: A Modern Introduction to Its Foundations* (Springer Cham, 2013) Chap. 6.
- [12] A. Bar-Shalom, M. Klapisch, and J. Oreg, Phase-amplitude algorithms for atomic continuum orbitals and radial integrals, *Computer Physics Communications* **93**, 21 (1996).
- [13] C. Froese-Fischer, T. Brage, and P. Jonsson, *Computational Atomic Structure An MCHF Approach* (Routledge, 1997) Chap. 10.
- [14] H. Bethe and E. Salpeter, *Quantum Mechanics of One- and Two-Electron Atoms* (Springer, 2014).
- [15] S. Kiyokawa, Exact solution to the Coulomb wave using the linearized phase-amplitude method, *AIP Advances* **5**, 087150 (2015), [https://pubs.aip.org/aip/adv/article-pdf/doi/10.1063/1.4929399/12899744/087150\\_1\\_online.pdf](https://pubs.aip.org/aip/adv/article-pdf/doi/10.1063/1.4929399/12899744/087150_1_online.pdf).
- [16] M. Seaton, Coulomb functions for attractive and repulsive potentials and for positive and negative energies, *Computer Physics Communications* **146**, 225 (2002).
- [17] GSL - GNU scientific library, <http://www.gnu.org/software/gsl/> (2010).